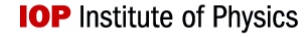
# **New Journal of Physics**

The open access journal at the forefront of physics





### **PAPER • OPEN ACCESS**

# One-dimensional magneto-optical compression of a cold CaF molecular beam

To cite this article: Eunmi Chae et al 2017 New J. Phys. 19 033035

View the article online for updates and enhancements.

# Related content

- Characteristics of a magneto-optical trap of molecules H J Williams, S Truppe, M Hambach et al.
- Laser slowing of CaF molecules to near the capture velocity of a molecular MOT Boerge Hemmerling, Eunmi Chae, Aakash
- Improved magneto-optical trapping of a diatomic molecule D J McCarron, E B Norrgard, M H Steinecker et al.

# Recent citations

- No evaporative cooling of nitric oxide in its ground state Lucie D. Augustoviov&#225 and and John L. Bohn
- Radio Frequency Magneto-Optical Trapping of CaF with High Density Loïc Anderegg et al

# **New Journal of Physics**

The open access journal at the forefront of physics



Published in partnership with: Deutsche Physikalische Gesellschaft and the Institute of Physics



#### **OPEN ACCESS**

#### RECEIVED

11 January 2017

#### REVISED

13 February 2017

# ACCEPTED FOR PUBLICATION

3 March 2017

#### PUBLISHED

27 March 2017

Original content from this work may be used under the terms of the Creative Commons Attribution 3.0

Any further distribution of this work must maintain attribution to the author(s) and the title of the work, journal citation and DOL



## PAPER

# One-dimensional magneto-optical compression of a cold CaF molecular beam

Eunmi Chae<sup>1,2,5</sup>, Loic Anderegg<sup>1,2</sup>, Benjamin L Augenbraun<sup>1,2</sup>, Aakash Ravi<sup>1,2</sup>, Boerge Hemmerling<sup>1,2,6</sup>, Nicholas R Hutzler<sup>1,2</sup>, Alejandra L Collopy<sup>3</sup>, Jun Ye<sup>3</sup>, Wolfgang Ketterle<sup>2,4</sup> and John M Doyle<sup>1,2</sup>

- Department of Physics, Harvard University, Cambridge, MA 02138, United States of America
- Harvard-MIT Center for Ultracold Atoms, Cambridge, MA 02138, United States of America
- <sup>3</sup> JILA, National Institute of Standards and Technology and University of Colorado, Boulder, CO 80309, United States of America
- Department of Physics, Massachusetts Institute of Technology, Cambridge, MA 02139, United States of America
- <sup>5</sup> Present address: Photon Science Center, School of Engineering, the University of Tokyo, Japan 113-8656.
- 6 Present address: Department of Physics, University of California, Berkeley, CA 94720, United States of America.

E-mail: eunmi@cua.harvard.edu

Keywords: laser cooling of molecules, molecular RF magneto-optical trap, cryogenic molecular buffer-gas beam

#### Abstract

We demonstrate the one-dimensional, transverse magneto-optical compression of a cold beam of calcium monofluoride (CaF). By continually alternating the magnetic field direction and laser polarizations of the magneto-optical trap (RF MOT), a photon scattering rate of  $2\pi \times 0.4$  MHz is achieved. A 3D model for this RF MOT, validated by agreement with data, predicts a 3D RF MOT capture velocity for CaF of 5 m s<sup>-1</sup>.

#### 1. Introduction

Molecules are intriguing candidates for the study of fundamental symmetry violation, quantum simulation of strongly correlated Hamiltonians, and the creation of new quantum information systems that take advantage of internal molecular degrees of freedom [1–10]. In addition, active research is ongoing to create cold molecules for new studies in order to understand the full role of quantum mechanics in chemical reactions [11, 12]. The main difficulty in pursuing these goals is to controllably prepare molecules in single quantum states, and to achieve long interaction times (typically achieved via trapping). Even the simplest molecules, diatomic molecules, have complex enough internal structure that, at room temperature, typically tens of thousands of states are thermally populated. Only very recently have molecular quantum states been controlled in a way to allow for quantum state-dependent chemical reactions [11, 12]. In that work, ultracold bi-alkali molecules were produced in a single quantum state by combining two ultracold alkali atoms, taking advantage of the mature, powerful tools for atom cooling [13–18]. However, this technique is so far limited to a specific subset of molecules, typically bialkalis in the  $^{1}\Sigma$  state. Extension of these methods to more chemically diverse species is a formidable challenge.

To fully utilize the powerful diversity of molecules, new methods to produce cold and ultracold molecules (e.g. those with electron spin degree of freedom) are desirable. A crucial step towards achieving lower temperatures is trapping, which in itself allows for further cooling methods to be applied. Major efforts are currently ongoing to trap molecules using electric, magnetic, and optical forces [19–31]. One promising option is a magneto-optical trap (MOT), the workhorse tool of optical cooling and confinement for atoms. Despite thorough study and understanding of atomic MOTs, the additional internal structure present in molecules has made it difficult to produce a molecular MOT, mostly due to the lack of closed cycling transitions. It is possible to overcome this difficulty by using molecules with sufficiently diagonal Franck—Condon factors (FCFs), as was proposed in [32, 33]. Recently, 2D and 3D MOTs for molecules have been realized with YO and SrF [34–37]. This scheme, although limited to molecules with strong optical transitions and highly diagonal FCFs, represents a powerful step toward broadening the scope of molecules that can be brought to the ultracold regime, including many which are of interest for new schemes in quantum simulation [6].

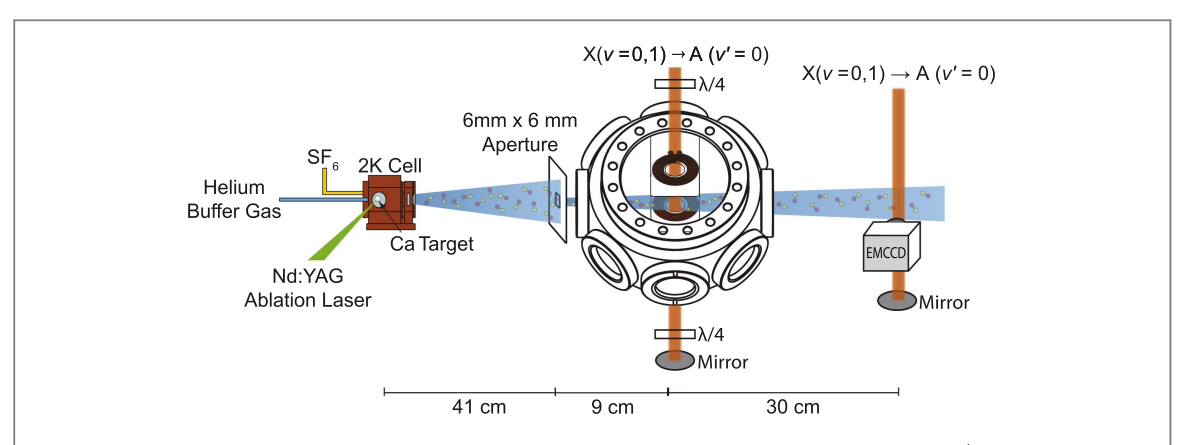


**Figure 1.** Experimental setup (not to scale). The cell where molecules are generated is cooled by a pumped liquid <sup>4</sup>He bath. An aperture of 6 mm  $\times$  6 mm is placed 41 cm downstream from the cell to collimate the molecular beam and to reduce the remaining <sup>4</sup>He buffer-gas. The molecules interact with the lasers 50 cm from the cell where the in-vacuum RF coils are in place. After the interaction, the molecules travel 30 cm farther and are detected by fluorescence with an electron multiplying charge-coupled device (EMCCD) camera. All lasers include X(v = 0, 1) - A(v' = 0) transitions and their hyperfine splittings.

CaF is a prototypical molecule for cold and ultracold applications and has been studied extensively, including its collisional properties [38–42]. It has an unpaired outer shell electron, strong laser cooling transitions, and reasonably diagonal FCFs. Furthermore, its light mass leads to a larger velocity change per photon scatter, which, compared to larger mass species with all other spectroscopic properties the same, shortens the slowing distance and increases the capture velocity of a MOT. It is therefore a molecule that is well suited for laser cooling. Using the X(v=0) - A(v'=0) transition at 606 nm with a linewidth of  $2\pi \times 8.29$  MHz [38], about  $10^5$  photons can be scattered with 2 vibrational repump lasers, before falling into higher vibrational states [43]. Recent theoretical work indicates that CaF is a good candidate for sympathetic/evaporative cooling to reach temperatures in the microkelvin regime, a necessary step toward quantum degeneracy [41, 42]. Once an ensemble of ultracold CaF molecules is prepared, its large electric dipole moment and spin degree of freedom will expand the Hamiltonians that can be simulated, including spin-lattice models [6].

Here we report a demonstration of magneto-optical compression of a CaF molecular beam. This is a key milestone towards loading CaF into a 3D MOT. This work verifies all of the processes and technology necessary for magneto-optical trapping of CaF, identifies an important MOT-limiting feature of CaF due to level crossings, and provides crucial data for validating RF MOT loading models. Our results also point towards the optimal parameters for achieving a RF MOT with a maximum number of trapped CaF molecules.

# 2. Methods

A schematic of the apparatus is depicted in figure 1. In our experiment, a cryogenic two-stage buffer-gas beam source is used to produce a cold CaF molecular beam [44–47]. CaF molecules are generated by ablating a metallic Ca target in an SF<sub>6</sub> ice environment within a copper cell, similar to the work in [48]. The molecules are cooled through collisions with He gas in a cell held at a temperature of around 2 K. Cold molecules and atomic He exit the cell aperture, forming a beam with a mean forward velocity of  $110 \pm 10$  m s<sup>-1</sup>, and velocity spread of 40 m s<sup>-1</sup>. To reduce the amount of buffer gas reaching the interaction region and to collimate the molecular beam, a 6 mm  $\times$  6 mm aperture is placed 41 cm from the cell, 9 cm before the molecules interact with the RF MOT magnetic fields and corresponding transverse laser beams. This aperture sets the molecular beam width in the detection area. In these experiments only a single MOT beam—transverse to the molecular beam—is used to quantitatively study the RF magneto-optical force in 1D [34]. After molecules pass through the interaction region, they travel about 30 cm farther where they are detected on an EMCCD (Andor, Luca R) using fluorescence.

The relevant energy levels of CaF are shown in figure 2. The optical transitions in use are from the electronic ground state X to the first electronic excited state A. The measured FCF for X(v=0)-A(v'=0) is 0.987 [38] and one vibrational repump laser from the v=1 state is used, allowing up to 1000 photons to be scattered before pumping of the molecules to the v=2 state [43]. Loss to other rotational states is prevented by addressing a J to J'=J-1 transition [33]. In this transition, the rotationally excited X(N=1) state is excited to the N'=0 state of the A state so that a combination of parity and angular momentum selection rules results in the A(N'=0) state molecules decaying back to the X(N=1) state.

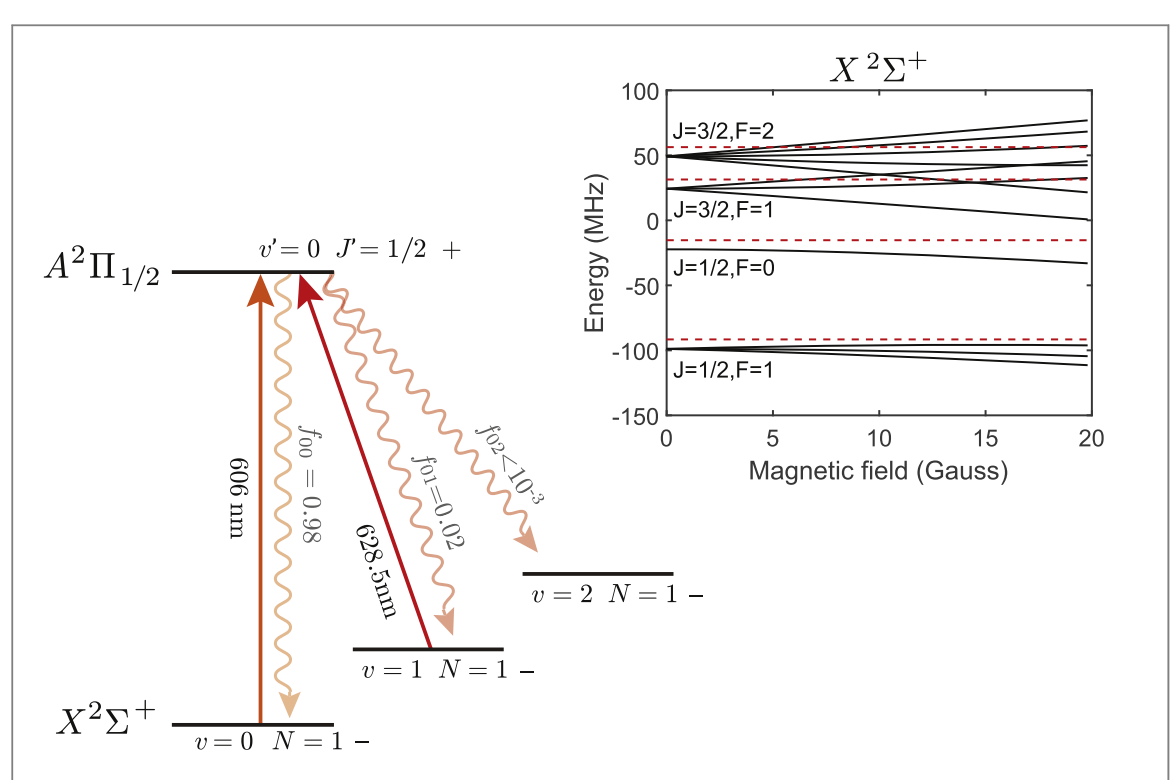


Figure 2. Level diagram for CaF molecules. Only relevant levels are shown. Quantum numbers for vibration, rotation, electronic angular momentum plus rotation, and the molecule's total angular momentum are v, N, J, and F respectively. The parity of the state is denoted by  $\pm$ . The straight lines indicate lasers used in the experiment and wavy lines show the decay from the excited states. FCFs  $(f_{ij})$  are also shown. The inset shows the hyperfine states and their Zeeman shift in the ground state X (v = 0, N = 1). The red-detuned laser frequencies are shown in red broken lines in the inset. The hyperfine splitting and the Zeeman shift of the excited state X (v = 0, V = 1/2) is negligible [39].

There are 4 hyperfine states that are spaced a few tens of MHz in the X(N=1) state manifold due to coupling of the electron's spin (S=1/2) with the molecular rotation (N=1) and fluorine's nuclear spin (I=1/2). This hyperfine splitting weakens the magneto-optical force in two ways: reduction of the scattering rate and level-crossing in weak magnetic fields at around 10 Gauss (figure 2 inset). All states are individually addressed through frequency sidebands placed on the lasers. One of the hyperfine states (I=1/2, I=1) has an opposite sign of the I=1/2 factor and the polarization of the lasers addressing this state has opposite handedness relative to the other states. The intensity of the I=1/2 factor I=1/2 factor and the polarization of the lasers addressing this state has opposite handedness relative to the other states. The intensity of the I=1/2 factor I

$$R_{\rm sc} = \Gamma \frac{n_e}{(n_g + n_e) + 2\sum_{i=1}^{n_g} (1 + 4\Delta_j^2/\Gamma^2) I_{{\rm sat},j}/I_j},\tag{1}$$

where  $\Gamma$  is a linewidth of the excited states ( $2\pi \times 8.29$  MHz [38]),  $n_g(n_e)$  is the number of involved states in the ground (excited) state manifold,  $\Delta_j$  is a laser detuning for the j state,  $I_{\text{sat},j}$  is a two-level saturation intensity for the j state (4.87 mW cm<sup>-2</sup> and 4.37 mW cm<sup>-2</sup> for the  $\nu=0$  and  $\nu=1$  states respectively), and  $I_j$  is laser intensity for the j state. The experimental parameters result in the scattering rate  $R_{\text{sc}} \sim 2\pi \times 0.43$  MHz from equation (1). The hyperfine splitting of the excited state A is unresolved [38].

One additional complication of a molecular MOT compared to an atomic MOT is that the number of involved ground magnetic substates is greater than that of the excited states. Because of this, some of the states become dark states of the confining lasers. The only way molecules could get out those states in a normal MOT would be scattering anti-confining photons, destroying the MOT effect. RF MOTs [34, 37] solve this problem by actively switching the magnetic field gradient and the polarization of the light synchronously at a rate comparable to the excited state's lifetime. With this scheme, molecules in all states predominantly scatter photons that lead to confinement and can be trapped. Switching of the lasers' polarizations is implemented using a Pockels cell. To switch the needed magnetic fields at a rate on the order of MHz, the coils are made small and internal to the vacuum chamber (figure 3). The coils are made out of a 0.85 mm thick copper sheet cut to a spiral coil shape with wire width of 1 mm on a 1.5 mm thick alumina substrate. The inner diameter of the coils is about 15 mm and there are 6 turns for each coil. There are 4 coils total, 2 on the upper board and 2 on the lower board

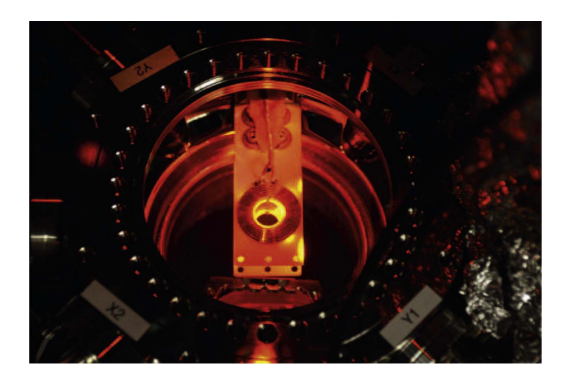


Figure 3. RF MOT coils inside the vacuum chamber. The picture was taken before the inside was blackened with a non conductive, low outgassing paint (MH2200 from Alion) to reduce the background scattered light.

—with the boards spaced by 16 mm. Coils on the same board are wired in a Helmholtz configuration, while the two boards together provide an anti-Helmholtz field in the space between them. Alumina was chosen due to its low outgassing rate (necessary for the UHV environment of the MOT) and good thermal conductivity (necessary to carry out the substantial heating produced when switching the coils at high frequencies). The alumina boards are mounted on an aluminum block, which is itself mounted to a copper block feedthrough. On the air-side of the feedthrough, we put a passive heatsink to further increase the cooling power. With this setup, we observe only a few degrees of temperature increase of the block feedthrough when running the coils in RF mode at 830 kHz. The coil assembly is connected to a resonant circuit outside of the chamber. With 1 Amp of current run through the coils, a quadrupole magnetic field of about 7.3 (3.7) Gauss cm<sup>-1</sup> is produced in the axial (radial) direction.

The molecules are detected by collecting fluorescent photons using an EMCCD camera. The excitation lasers (X(v=0, 1) - A(v'=0)) cross the molecular beam at 90 degrees in the detection region, 80 cm downstream from the source. The measured width of the molecular beam is a convolution of the transverse velocity of the beam and the initial beam spread. We analyze this molecular beam width to infer the compression and cooling effect from the magneto-optical force.

# 3. Results and discussion

Figures 4 and 5 show the compression of the molecular beam by the magneto-optical force. Typical molecular beam signals with red-detuned X(v=0)-A(v'=0) lasers when the magnetic field and the light polarization are in phase and out of phase are depicted in figure 4. The magneto-optical compression narrows the molecular beam when the phase of the magnetic field and the light polarization are matched. In the opposite condition with the relative phase of 180°, the molecular beam experiences an anti-confining force and its width is increased. The measured beam profiles are fit using super-Gaussian functions of order 4 with their amplitudes, beam widths as given by the 1/e radius of a fit, and centers as free parameters.

The fitted beam widths are plotted in figure 5. Each data point in figure 5 is the average of 350 measurements (molecular pulses) for the red-detuned magneto-optical compression and Doppler cooling (figure 5(a)), and 200 (800) measurements for the blue-detuned magneto-optical compression (Doppler heating) (figure 5(b)). The relative phase between the polarization and the magnetic field is changed between each data point. Error bars indicate one-standard-deviation statistical uncertainties from fits to beam profiles. In the absence of the magnetic field, Doppler cooling (heating) is observed with red (blue)-detuning of lasers. The direction of the magneto-optical force is seen to reverse with blue-detuning of the lasers compared to the case with red-detuning as expected.

We have created Monte-Carlo simulations of the RF MOT similar to that described in [34]. The results of these simulations are shown in figure 5 as solid lines with scattering of 150 photons, corresponding to a photon scattering rate of  $2\pi \times 0.4$  MHz. This agrees with the expected scattering rate based on the measured laser powers and transition strengths. Due to the asymmetric hyperfine structure of CaF, a Monte-Carlo simulation with only one effective detuning gives good agreement for the red-detuning, while results are in worse agreement for the blue-detuned case. The widths of the molecular beam in the detection region for different conditions are summarized in figure 6.

At a detuning of 7 MHz, the optimal compression is achieved with a magnetic field gradient of 7.3 Gauss cm<sup>-1</sup>. Several other field gradients (3.7, 4.4, 5.8, 12.4, and 18.3 Gauss cm<sup>-1</sup>) were tested but the compression effects are reduced compared to the optimal gradient. This is due to the small hyperfine splitting of CaF. Specifically, in a

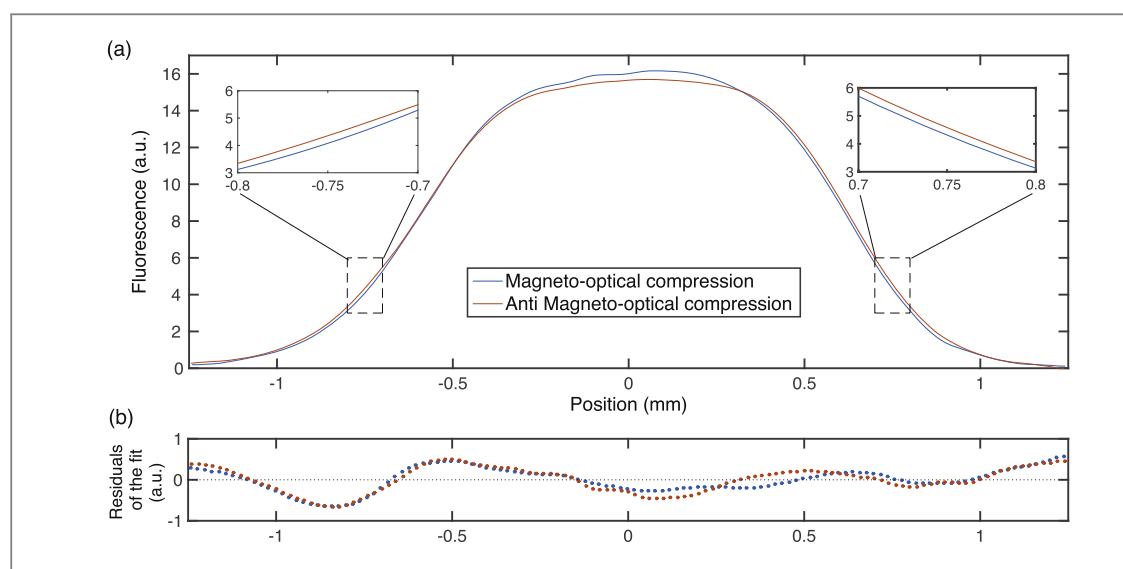


Figure 4. (a) Typical beam data with red-detuned lasers. The transverse beam shape after (anti) magneto-optical compression is depicted as a (red) blue line. The two configurations are achieved by changing the phase of the magnetic fields by  $180^{\circ}$ . The integrated area of the beam is conserved for the both cases. (b) The residuals of the fits to super-Gaussian functions are shown. The vertical unit is same as in (a). Due to the original beam shape that is skewed to the leftside, the residuals differ from zero on the edges of the beams, as expected. However, the residuals of the MOT and the anti-MOT data are equal to a level smaller than the average shift where the profile is most sensitive, the wings and peak. This assures that the fitting is a valuable quantitative evaluation of the magneto-optical compression.

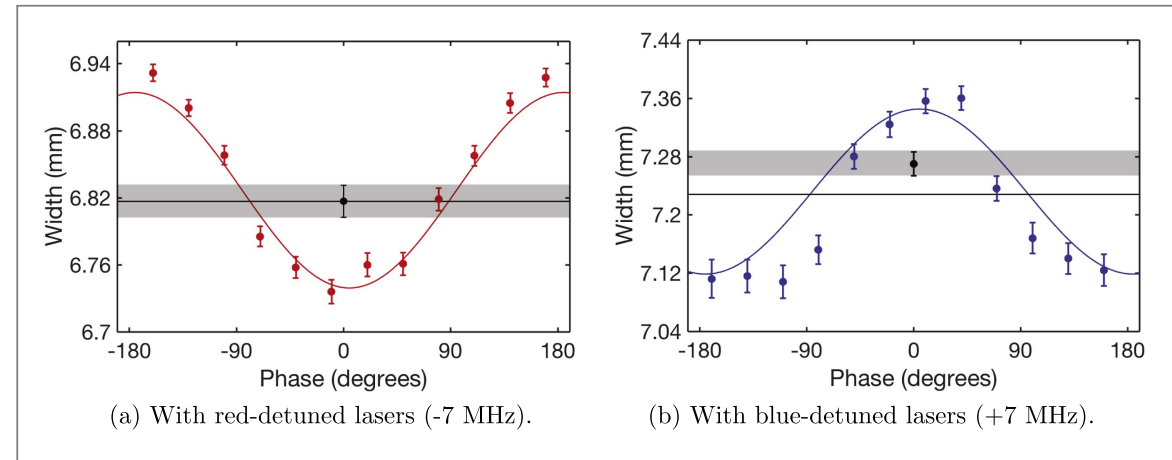
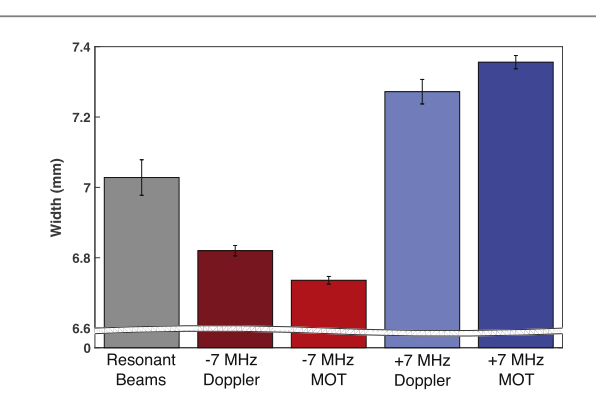


Figure 5. Molecular beam widths are plotted as a function of the relative phase between the magnetic field and the polarization of the lasers: red dots in (a) for the  $X(\nu=0)-A(\nu=0)$  laser detuning of -7 MHz, and blue dots in (b) for the  $X(\nu=0)-A(\nu=0)$  laser detuning of +7 MHz. The black dot in each figure indicates the beam width when the MOT coils were switched off and reflects the effect of Doppler cooling or heating. Gray area is a guide to eyes, indicating the  $\pm 1\sigma$  confidence region of the Doppler width. Error bars are one-standard-deviation statistical uncertainties from fits to beam profiles. Lines show the Monte-Carlo simulation results for each case.

magnetic field greater than 5 Gauss, the energy difference between magnetic sublevels of different hyperfine states approaches the natural linewidth. This increases the probability of scattering anti-confining photons, and thus weakens the compression effect.

The 1D magneto-optical compression demonstrated here provides us with an improved understanding of the 3D MOT for CaF. Using the number of scattered photons in 1D magneto-optical compression, simple calculations estimate a maximum (on-axis, perfect conditions) capture velocity of about 13 m s $^{-1}$  for the 3D MOT in this experimental setup with our current geometry and a fairly generic laser configuration for the *X*–*A* transition. We have also performed a full 3D MOT Monte-Carlo simulation of trap loading for both on-axis and the more realistic set of molecular trajectories that include off-axis molecules. Considering the limiting case of molecules entering the MOT region only directly on-axis with the zero magnetic field point of the MOT, the capture velocity is seen in the simulation to be 10 m s $^{-1}$ , which agrees with the simple calculation. However, since the capture velocity decreases as the molecules travel off axis, we find that the averaged capture velocity is about half of the ideal on-axis estimation, resulting in an effective capture velocity (simulating the molecular beam as a whole, including off-axis trajectories) of about 5 m s $^{-1}$  for the molecular beam as a whole. White-light slowing of



**Figure 6.** Summary of the molecular beam width for each case. Both magnetic fields and detuned lasers are applied for the 'MOT' cases, while no magnetic fields are applied for the 'Doppler' cases. Molecular beam width after the molecules interacting with resonant lasers is shown for comparison. The error bars indicate one-standard-deviation statistical uncertainties from fits to beam profiles.

a CaF molecular beam demonstrated previously in our group [47] resulted in about  $5 \times 10^4$  molecules at  $5 \pm 4$  m s<sup>-1</sup> detected in the capture volume of the MOT. We expect a good fraction of these molecules would be captured in a RF MOT with current techniques.

# 4. Conclusion

Magneto-optical compression of a buffer-gas cooled CaF beam has been achieved. By scattering 150 photons during the time molecules spend in the RF MOT region (about 60  $\mu$ s), the molecular beam is compressed, in good agreement with our first principles model. From the demonstrated molecular beam compression, we estimate a RF MOT capture velocity of 5 m s<sup>-1</sup> for CaF.

This work provides a deeper understanding of the magneto-optical forces on CaF molecules and guides the necessary experimental conditions for effective loading of molecular MOTs. It further demonstrates the generality of the RF MOT scheme for molecules by adding an additional entry to the list of molecules on which magneto-optical forces have been demonstrated.

# Acknowledgments

This work was supported by the ARO, the CUA, and the NSF. BLA is supported by the National Science Foundation Graduate Research Fellowship under NSF Grant No. DGE1144152.

# References

- [1] Carr L D, DeMille D, Krems R V and Ye J 2009 New J. Phys. 11 055049
- [2] Baron J et al 2014 Science 343 269
- [3] DeMille D, Cahn SB, Murphree D, Rahmlow DA and Kozlov MG 2008 Phys. Rev. Lett. 100 023003
- [4] Baranov M A, Dalmonte M, Pupillo G and Zoller P 2012 Chem. Rev. 112 5012
- [5] Buchler HP, Demler E, Lukin M, Micheli A, Prokofev N, Pupillo G and Zoller P 2007 Phys. Rev. Lett. 98 060404
- [6] Micheli A, Brennen G K and Zoller P 2006 Nat. Phys. 2 341
- [7] Yan B, Moses SA, Gadway B, Covey JP, Hazzard KRA, Rey AM, Jin DS and Ye J 2013 Nature 501 521
- [8] André A, DeMille D, Doyle J M, Lukin M D, Maxwell S E, Rabl P, Schoelkopf R J and Zoller P 2006 Nat. Phys. 2 636
- [9] DeMille D 2002 Phys. Rev. Lett. 88 067901
- [10] Rabl P, DeMille D, Doyle J M, Lukin M D, Schoelkopf R J and Zoller P 2006 Phys. Rev. Lett. 97 033003
- [11] Ni K-K, Ospelkaus S, Wang D, Quéméner G, Neyenhuis B, de Miranda M H G, Bohn J L, Ye J and Jin D S 2010 Nature 464 1324
- [12] Ospelkaus S, Ni K-K, Wang D, de Miranda M H G, Neyenhuis B, Quéméner G, Julienne P S, Bohn J L, Jin D S and Ye J 2010 Science 327 853
- [13] Ni K-K, Ospelkaus S, de Miranda M H G, Pe'er A, Neyenhuis B, Zirbel J J, Kotochigova S, Julienne P S, Jin D S and Ye J 2008 Science
- [14] Moses S A, Covey J P, Miecnikowski M T, Yan B, Gadway B, Ye J and Jin D S 2015 Science 350 659
- [15] Park J W, Will S A and Zwierlein M W 2015 Phys. Rev. Lett. 114 205302
- [16] Takekoshi T, Reichsöllner L, Schindewolf A, Hutson J M, Le Sueur C R, Dulieu O, Ferlaino F, Grimm R and Nägerl H C 2014 *Phys. Rev. Lett.* 113 205301
- [17] Molony P K, Gregory P D, Ji Z, Lu B, Köppinger M P, Le Sueur C R, Blackley C L, Hutson J M and Cornish S L 2014 Phys. Rev. Lett. 113 255301
- [18] Guo M, Zhu B, Lu B, Ye X, Wang F, Vexiau R, Bouloufa-Maafa N, Quéméner G, Dulieu O and Wang D 2016 Phys. Rev. Lett. 116 205303
- [19] Hummon M, Tscherbul T, Klos J, Lu H-I, Tsikata E, Campbell W, Dalgarno A and Doyle J M 2011 Phys. Rev. Lett. 106 053201
- [20] Bethlem H L, Berden G, Crompvoets F M, Jongma R T, van Roij A J and Meijer G 2000 Nature 406 491

- [21] van de Meerakker S, Smeets P, Vanhaecke N, Jongma R and Meijer G 2005 Phys. Rev. Lett. 94 023004
- [22] Hoekstra S, Metsälä M, Zieger P, Scharfenberg L, Gilijamse J, Meijer G and van de Meerakker S 2007 Phys. Rev. A 76 063408
- [23] Zeppenfeld M, Englert B G U, Glöckner R, Prehn A, Mielenz M, Sommer C, van Buuren L D, Motsch M and Rempe G 2012 Nature 491 570
- [24] Prehn A, Ibrügger M, Glöckner R, Rempe G and Zeppenfeld M 2016 Phys. Rev. Lett. 116 063005
- [25] Weinstein J D, DeCarvalho R, Guillet T, Friedrich B and Doyle J M 1998 Nature 395 148
- [26] Sawyer B C, Lev B L, Hudson E R, Stuhl B K, Lara M, Bohn J L and Ye J 2007 Phys. Rev. Lett. 98 253002
- [27] Campbell W C, Tsikata E, Lu H-I, van Buuren L D and Doyle J M 2007 Phys. Rev. Lett. 98 213001
- [28] Lu H-I, Kozyryev I, Hemmerling B, Piskorski J and Doyle J M 2014 Phys. Rev. Lett. 112 113006
- [29] Stuhl B K, Hummon M T, Yeo M, Quéméner G, Bohn J L and Ye J 2012 Nature 492 396
- [30] Stoll M, Bakker J, Steimle T, Meijer G and Peters A 2008 Phys. Rev. A 78 032707
- [31] Riedel J, Hoekstra S, Jäger W, Gilijamse J J, Meerakker S Y T and Meijer G 2011 Eur. Phys. J. D 65 161
- [32] Rosa M D 2004 Eur. Phys. J. D 31 395
- [33] Stuhl B K, Sawyer B C, Wang D and Ye J 2008 Phys. Rev. Lett. 101 243002
- [34] Hummon MT, Yeo M, Stuhl BK, Collopy AL, Xia Y and Ye J 2013 Phys. Rev. Lett. 110 143001
- [35] Barry J F, McCarron D J, Norrgard E B, Steinecker M H and DeMille D 2014 Nature 512 286
- [36] McCarron D J, Norrgard E B, Steinecker M H and DeMille D 2015 New J. Phys. 17 035014
- [37] Norrgard E B, McCarron D J, Steinecker M H, Tarbutt M R and DeMille D 2016 Phys. Rev. Lett. 116 063004
- [38] Wall T, Kanem J, Hudson J, Sauer B, Cho D, Boshier M, Hinds E and Tarbutt M R 2008 Phys. Rev. A 78 062509
- [39] Devlin J, Tarbutt MR, Kokkin DL and Steimle TC 2015 J. Mol. Spectrosc. 317 1
- [40] Maussang K, Egorov D, Helton J S, Nguyen S V and Doyle J M 2005 Phys. Rev. Lett. 94 123002
- [41] Lim J, Frye M D, Hutson J M and Tarbutt M R 2015 Phys. Rev. A 92 053419
- [42] Quéméner G and Bohn J L 2016 Phys. Rev. A 93 012704
- [43] Pelegrini M, Vivacqua C S, Roberto-Neto O, Ornellas FR and Machado FB C 2005 Braz. J. Phys. 35 950
- [44] Lu H-I, Rasmussen J, Wright MJ, Patterson D and Doyle J M 2011 Phys. Chem. Chem. Phys. 13 18986
- [45] Hutzler NR, Lu H-I and Doyle JM 2012 Chem. Rev. 112 4803
- [46] Hemmerling B, Drayna G K, Chae E, Ravi A and Doyle J M 2014 New J. Phys. 16 063070
- [47] Hemmerling B, Chae E, Ravi A, Anderegg L, Drayna G K, Hutzler N R, Collopy A L, Ye J, Ketterle W and Doyle J M 2016 J. Phys. B: At. Mol. Opt. Phys. 49 174001
- [48] Williams H, Tarbutt MR and Sauer B E 2015 private conversation